ORIGINAL ARTICLE
Iran J Allergy Asthma Immunol
In press.

Alterations in Apoptotic Cell Populations, Protein Markers, and Gene Expression Patterns in Rats with Sulfur Mustard-induced Pulmonary Injuries

Tao Liu[1], Na Zhang[1], Xin Shu[2], Xiaoxuan Hu[3,4], Jingtong Li[1], Yuxu Zhong[4], Jinyuan Tang[1], and Xiao-ji Zhu[1]

[1] Department of Respiration, The 80th Group Army Hospital of People's Liberation Army, Weifang, China
[2] Department of Dermatology, The Third Medical Center of Chinese PLA General Hospital, Beijing, China
[3] Department of Pulmonary and Critical Care Medicine, Weifang No. 2 People's Hospital, Weifang, China
[4] Institute of Toxicology and Pharmacology, Academy of Military Medical Sciences, Beijing, China

Received: 6 April 2025; Received in revised form: 11 August 2025; Accepted: 20 August 2025

ABSTRACT

Sulfur mustard (SM) is a potent chemical warfare agent that causes severe cutaneous, ocular, and pulmonary injuries, with respiratory tract damage being the most life-threatening. Despite its well-documented toxicity, the cellular mechanisms driving SM-induced apoptosis remain poorly understood. This study seeks to elucidate the apoptotic pathways involved in SM-induced pulmonary injury using a rat model.

We induced acute lung injury through two delivery methods: intraperitoneal injection (8 mg/kg) and intratracheal instillation (2 mg/kg) of SM, with both doses representing 1 LD_{50}. We assessed apoptosis-related proteins and gene expression through TUNEL staining, immunohistochemistry, and quantitative real-time PCR analyses.

Intraperitoneal administration of SM resulted in significantly elevated expression of apoptotic markers including annexin A1, annexin A2, cytochrome C, caspase-12, and JNK3, in alveolar epithelial cells compared to intratracheal delivery. Both TUNEL assays and immunohistochemical staining confirmed these findings. These results indicate that intraperitoneal SM exposure triggers more severe apoptotic responses in alveolar epithelial cells than intratracheal exposure at equivalent doses.

These findings demonstrate that intraperitoneal models can effectively identify apoptosis-related molecular targets suitable for therapeutic development.

Keywords: Acute pulmonary injury; Apoptosis; Equal lethal dose; Sulfur mustard

INTRODUCTION

Sulfur mustard (SM), as a vesicant, is often referred to as the "king of poison gases." Upon exposure, SM rapidly penetrates mucous membranes and induces severe damage to vital organs such as the skin, lungs,

Corresponding Authors: Xiao-ji Zhu, MD;
Department of Respiration, the 80th Group Army Hospital of People's Liberation Army, Weifang, China. Tel/Fax: (+860 536) 5019133, Email: xiaojizhu@163.com

Jinyuan Tang, MD;
Department of Respiration, the 80th Group Army Hospital of People's Liberation Army, Weifang, China. Tel/Fax: (+860 536) 5019133, Email: hnmrtjy981@163.com

*The first two authors contributed equally to this work.

Published by Tehran University of Medical Sciences (http://ijaai.tums.ac.ir)

and eyes.[1] It acts as a bifunctional alkylating agent and forms sulfonium ions upon contact with body fluids, targeting DNA/proteins; this interstrand cross-linking directly blocks replication, whereas monoalkylation induces mutation accumulation; the resultant DNA damage is irreversible and cannot be repaired.[2] The respiratory system is a primary target and the major route after SM's exposure. The inhalation of SM vapor is lethal and may lead to chronic respiratory dysfunction and long-term disability in the survivors.[3] Consequently, extensive research has focused on elucidating the mechanisms underlying the SM-induced toxicity, which possibly involves DNA damage, glutathione depletion, oxidative stress, apoptosis, inflammation, lipid peroxidation, and protein dysfunction.

The primary molecular mechanisms through which SM induces cytotoxicity involve multiple apoptotic pathways. As a bifunctional alkylating agent, SM forms DNA cross-links, thereby disrupting DNA replication and transcription and activating DNA damage-response pathways. The DNA damage then triggers the ATM-Chk2-p53-signaling pathway, which activates p53 and subsequently promotes the expression of Bcl-2-associated X protein (Bax) and programmed cell death protein 4, along with other cytotoxic mediators. The activation of Bax and BCL-2 antagonist killer 1 (Bak) promotes their oligomerization in the mitochondrial outer membrane, forming pores that increase the membrane permeabilization and trigger the release of cytochrome c (Cyt C) from the mitochondrial intermembrane space into the cytoplasm. This intrinsic apoptotic pathway is initiated by the Cyt C release from the mitochondria, which then forms a heptameric complex with apoptotic protease-activating factor-1 in a dATP-dependent manner. The resulting complex activates caspase-9, which, in turn, initiates the activation of downstream effector caspases-3 and -7, executing the apoptotic process. Concurrently, glutathione depletion reduces antioxidant capacity, whereas the accumulation of reactive oxygen species creates a vicious cycle that exacerbates mitochondrial dysfunction and DNA damage. The unfolded protein response, particularly through protein kinase R-endoplasmic reticulum kinase-signaling pathway and inositol-requiring enzyme 1 alpha activation, further promotes apoptosis.

In addition, inflammatory cytokines can initiate the extrinsic apoptotic pathway through tumor necrosis factor receptor-1/Fas-associated death domain/caspase-8 signaling. Excessive autophagy may also contribute to apoptosis, for instance, through the dissociation of Beclin-1 from Bcl-2.[4,5] Key molecular targets of SM include DNA repair enzymes [e.g., poly (ADP-ribose) polymerase, X-ray repair cross-complementing group 1], apoptosis regulators (e.g., p53, Bax/Bak, Bcl-2 family), and inflammatory mediators (e.g., nuclear factor-κB, tumor necrosis factor-α). Consequently, therapeutic strategies targeting antioxidants, poly (ADP-ribose) polymerase inhibitors, and caspase inhibition are being explored toward the prevention and intervention of SM-induced toxicity.[6,7]

Previously, two acute pulmonary injury models were established in murine models using SM to investigate inflammatory and oxidative stress responses.[8,9] To further investigate the apoptotic mechanisms mediated by SM, we performed terminal deoxynucleotidyl transferase dUTP nick-end labeling (TUNEL) staining, immunohistochemical labeling, and quantitative real-time PCR to monitor apoptosis-related changes in the lung tissues following SM exposure. Comparison of the effects of intraperitoneal injection and intratracheal instillation led to the identification of significant differences in apoptotic responses, thereby providing insight for the development of targeted interventions in SM-induced pulmonary injury.

MATERIALS AND METHODS

Reagents and Instruments

The following reagents were used in the study: SM (CAS 505-60-2; 99% pure; Academy of Military Medical Sciences, China); absolute ethanol solution (Cat #E130059; pure 99.7%; Shanghai Aladdin Biochemical Technological Co., Ltd., Shanghai, China); annexin A1 and annexin A2 immunohistochemical kits (Cat #ab196830, Cat #ab178677; Abcam Co., Ltd., Cambridge, MA, USA); Cyt C and cysteinyl aspartate specific proteinase-12 (caspase-12) (Cat #K006612P, Cat #K001602P; Solarbio Co., Ltd., Beijing, China); c-Jun N-terminal kinase3 (JNK3) immunohistochemical kits (Cat #NBP2-61801; Novus Biologicals Co., Ltd., Rochester Hills, MI, USA); protease K, apop A, and apop B (Roche Biotechnology Company, Basel, Switzerland). SYBR PrimeScript RT-PCR Kit II and primer sequences (designed and synthesized by Solarbio Co., Ltd.); fluorescence quantitative PCR (Bio-RadIQ5; Bio-Rad, Hercules, CA, USA); an automatic analyzer (ProteinSimple Ltd., Silicon Valley, CA, USA)

equipped with Pannoramic P250 (3DHIESTECH Co., Ltd., Budapest, Hungary).

Experimental Protocol

A total of 236 male Sprague–Dawley rats, specific pathogen-free (weight: 280–300 g, age: 15 weeks), were purchased from the Animal Center of Academy of Military Medical Sciences (Certification No. 0015902; Beijing, China). Subsequently, 136 of them were randomly assigned to the following groups: experimental (intraperitoneal SM [n = 32]; intratracheal SM [n = 32]); placebo (intraperitoneal absolute ethanol-control [n = 32]; intratracheal absolute ethanol-control [n = 32]); untreated control (n = 8). SM was diluted in absolute ethanol for subsequent analyses. The proportions of SM and absolute ethanol were SM (0.00157 mmol) in absolute ethanol (0.1 mL). To establish an intratracheal instillation model, the experimental rats were housed in a separate room and exposed to 12 hours of photophase at 24 ± 2°C under 60–65% relative humidity. The rats received a standard diet of food and water. Each rat was subcutaneously injected with atropine (0.05 mg/kg) and then anesthetized via an intraperitoneal administration of ketamine hydrochloride (100 mg/kg) after 30 minutes.[8] For the SM group, 0.1 mL of the SM solution (0.98 LD_{50}=2 mg/kg) was instilled into the trachea of each rat and flushed with 0.1 mL of air. After catheter withdrawal, the animals were placed in the ventral position on a heating pad within a small chamber. Supplemental oxygen was provided initially at 100% and gradually weaned to 21% over 20 minutes. The animals were monitored for signs of respiratory distress for 4 hours following this intervention, after which the rats were returned to their cage. In the intratracheal absolute ethanol-control group, 0.1 mL of absolute ethanol was instilled into the trachea.

To establish an animal model of intraperitoneal injection, the rats in this group were anesthetized following the protocol described earlier. SM (0.1 mL/rat [0.96 LD_{50}=8 mg/kg]) was intraperitoneally administered into SM rats, whereas absolute ethanol (0.1 mL/rat) was administered intraperitoneally to absolute ethanol-control rats.[8] The control rats received no treatment.

For establishing an acute pulmonary injury model via intraperitoneal injection and intratracheal instillation, a pilot study was conducted in 100 rats to determine the LD_{50} of SM using Horn's method. The LD_{50} dose was then calculated based on the mortality outcomes.[9]

Animal Euthanasia and Specimen Collection

At 6, 24, 48, and 72 hours following the last SM exposure, the rats were euthanized via an intraperitoneal injection of pentobarbital sodium (150 mg/kg) in accordance with the institutional animal care guidelines. After 15–30 minutes, euthanasia was confirmed by the cessation of cardiac and respiratory function. The lung (right-lower lobe) of the rats was then removed for biochemical analyses. The lung tissue specimen was fixed in 10% formaldehyde, dehydrated through a graded alcohol series, cleared with xylene, embedded in paraffin, and then sliced into 4-μm-thick serial slices. These sections were then analyzed immunohistochemically.[10] Fresh tissues were preserved in liquid nitrogen until PCR analysis.

TUNEL Staining

For TUNEL labeling, the aforementioned paraffin sections (4-μm) were dewaxed and rehydrated, subjected to proteinase K treatment, and then fixed and permeabilized. The TUNEL reaction solution was prepared, and the sections were incubated in it. Negative and positive controls were set. The sections were subjected to fluorescence labeling. Cells showing brown granules in the nucleus or cytoplasm under epi-fluorescence microscopes were identified as apoptotic cells.[11]

Immunohistochemistry

The streptavidin-peroxidase method was used to treat the cells with primary monoclonal antibodies (i.e., annexin A1, annexin A2, Cyt C, caspase-12, and JNK3) diluted 1:50, followed by that with sheep anti-mouse/rabbit IgG polymer secondary antibody (Cat #ZF0314; diluted in 1:100).[11] Observations were conducted under high-power magnification (×400), with a minimum of five high-power fields examined per section. The proportion of positive cells for the alveolar septa was calculated as follows: positive cells/total cells in five high-power fields×100%. Finally, the mean value of the proportion of positive cells was determined.

Measurement of Annexin A1, Annexin A2, Cyt C, Caspase-12, and JNK3 mRNA Expression by Fluorescence Quantitative PCR

Pulmonary tissues from each group of rats were homogenized in Trizol reagent as per the manufacturer's instructions. Total RNA was extracted and dissolved in diethyl pyrocarbonate-treated water and then stored at -

80°C until further use. Target gene-specific primers (0.2 μM) and β-actin primers were used for normalization in qPCR. RNase-free water served as a no-template negative control to exclude contamination (Table 1).[11]

Table 1. Primer sequences and amplified fragment lengths of annexin A1, annexin A2, Cyt C, caspase-12, and JNK3

Gene	Genebank Accession	Primer	Amplified fragment length
Annexin A1	NM_012904.2	Upstream：5′- CTGGAGGAGGTTGTTTTGGC -3′ Downstream：5′- GAGCAAGCAAGGCATTACGA -3′	238 bp
Annexin A2	NM_019905.1	Upstream：5′- ATCATCTGCTCAAGAACCAACC -3′ Downstream：5′- CTGCCCGTTTACCCTTTGC -3′	151 bp
Cyt C	NM_012839.2	Upstream：5′- CCCTAAGAGTCTGATCCTTTGTG -3′ Downstream：5′- TCCAGTCTTATGCTTGCCTC -3′	141 bp
Caspase-12	NM_130422.1	Upstream：5′- TGGAAGGTAGGCAAGAGTGG-3′ Downstream：5′- AAGGTAGAAGTAGCGTGTCATAG -3′	183 bp
JNK3	NM_001270556.1	Upstream：5′- GTGATGGAACTGATGGAC -3′ Downstream：5′- TTGACTACGATGTTACTGG -3′	161 bp
β-Actin	NM_031144.3	Upstream：5′- TAAGGCCAACCGTGAAAAGAT Downstream：5′- GGTACGACCAGAGGCATACA	109 bp

caspase-12: cysteinyl aspartate specific proteinase-12; Cyt C: cytochrome c; JNK3: c-Jun N-terminal kinase 3.

Statistical Analyses

All statistical analyses were conducted using SPSS 25.0 software. Normality was tested by the Shapiro–Wilk test, and homogeneity of variance was assessed by Levene's test. Data are presented as the mean ± standard deviation. Two-way ANOVA was used to evaluate the effects of the treatment route and time point on the measured outcomes. Subsequent Tukey HSD post-hoc tests were performed for multiple comparisons. To control the family-wise error rate in multiple comparisons, Bonferroni correction was applied to pairwise post-hoc tests. A p value<0.05 indicated statistical significance.

RESULTS

Positive Expression in Apoptotic Cells and Annexin A1, Annexin A2, Cyt C, Caspase-12, and JNK3 Proteins

Following SM exposure via both intraperitoneal and intratracheal pathways, apoptotic cells and key proteins (annexin A1, annexin A2, Cyt C, caspase-12, and JNK3) exhibited diffuse distribution throughout the alveolar septal epithelium at 6 and 24 hours post-exposure. However, by 48–72 hours, these cellular markers had reorganized into distinct clusters (Supplemental Figures 1–6). Control groups receiving intraperitoneal or intratracheal absolute ethanol, as well as untreated controls, showed sparse, uniform distribution of these markers across lung tissue throughout all time points (Figures 1A–H and 2A–H).

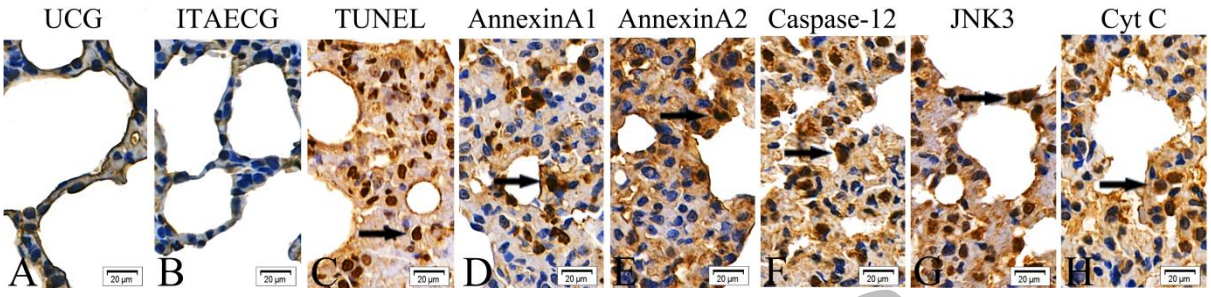

Figure 1. The expressions of apoptotic cells and annexin A1, annexin A2, caspase-12, JNK3, and Cyt C proteins in the alveolar septa of rats via intratracheal administration. ITSMG rats received intratracheal instillation of diluted SM (1LD$_{50}$=2 mg/kg). Panels A and B demonstrate the absence of apoptotic cells and protein labeling in ITAECG, consistent with findings in UCG. Panels C-H show pronounced apoptotic cell and protein labeling at 72 hours post-exposure in the SM-treated group, including TUNEL-positive cells and immunoreactivity for annexin A1, annexin A2, caspase-12, JNK3, and Cyt C (×400 magnification, scale bar=20 µm). caspase-12: cysteinyl aspartate specific proteinase-12; Cyt C: cytochrome c; ITECG: intratracheal ethanol-control group; ITSMG: intratracheal sulfur mustard group; JNK3: c-Jun N-terminal kinase3; TUNEL: terminal deoxynucleotidyl transferase dUTP nick-end labeling; UCG: untreated control group.

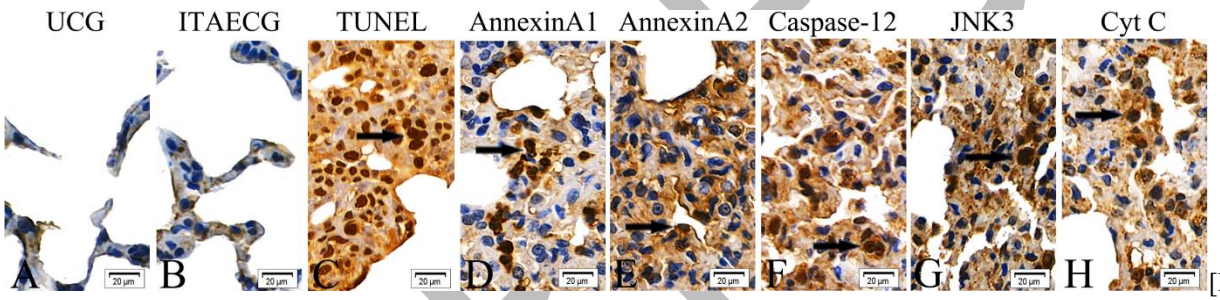

[Image

Figure 2. The expressions of apoptotic cells and annexin A1, annexin A2, caspase-12, JNK3: and Cyt C proteins in the alveolar septa of rats via intraperitoneal administration. IPSMG rats received an intraperitoneal injection of diluted SM (1LD$_{50}$=8 mg/kg). Panels A and B demonstrate the absence of apoptotic cells and protein labeling in IPAECG, consistent with findings in UCG. Panels C-H show pronounced apoptotic cell and protein labeling (arrows) at 72 hours post-exposure in IPSMG, including TUNEL-positive cells and immunoreactivity for annexin A1, annexin A2, caspase-12, JNK3, and Cyt C (×400 magnification: scale bar=20 µm). IPECG: intraperitoneal ethanol-control group; IPSMG: intraperitoneal sulfur mustard group.

Quantification of Apoptotic Marker Expression

Proportions of annexin A1-, annexin A2-, Cyt C-, caspase-12-, and JNK3-positive cells within alveolar septa were quantified across all groups using repeated measures ANOVA at multiple time points. Analysis revealed several key findings. Both intraperitoneal SM group (IPSMG) and intratracheal SM group (ITSMG) demonstrated significantly elevated proportions of positive cells at all measured time points, with statistically significant time-dependent increases throughout the study period. When compared to their respective ethanol control groups (ECG) and untreated control group (UCG), both SM exposure routes produced significantly higher proportions of positive cells in alveolar septa. IPSMG showed particularly pronounced increases over time (Figures 3A–E, 4A–E, and 5A–E).

mRNA Expressions of Annexin A1, Annexin A2, Cyt C, Caspase-12, and JNK3

The mRNA expressions of annexin A1, annexin A2, Cyt C, caspase-12, and JNK3 in the alveolar septal epithelial cells were analyzed across five groups using repeated measures ANOVA at multiple time points. The key observations are as follows: The mRNA expressions were significantly increased in the epithelial cells of the

Published by Tehran University of Medical Sciences (http://ijaai.tums.ac.ir)

alveolar septa in IPSMG and ITSMG at all time points. A statistically significant upward trend was recorded in the mRNA expression in both IPSMG and ITSMG. IPSMG exhibited significantly higher mRNA expression when compared to both ECG and UCG. ITSMG also exhibited significantly elevated mRNA levels when compared to controls, with a progressive increase in apoptosis-related gene expression over time, as shown in Figures 6A–E, 7A–E, and 8A–E.

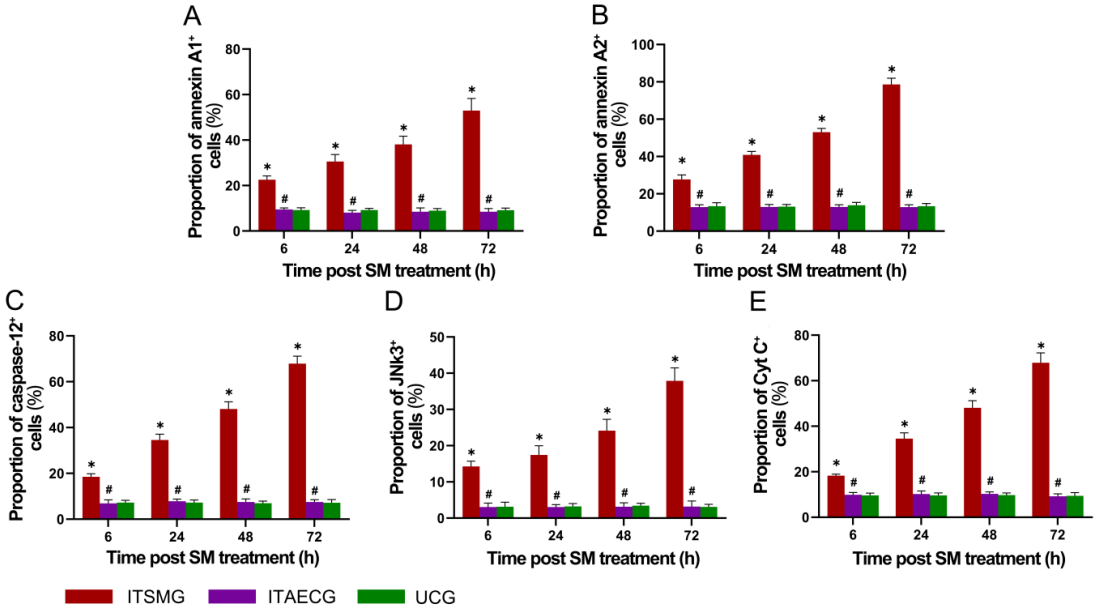

Figure 3. The proportion of annexin A1- (A), annexin A2- (B), caspase-12- (C), JNK3- (D), and Cyt C- (E) positive cells in the alveolar septa of rats via intratracheal administration. Figure 1 displays the rat treatment protocol. Data are mean ± SD, n=8. *p<0.05, compared with ITECG and UCG. #p>0.05, compared with untreated control group (UCG).

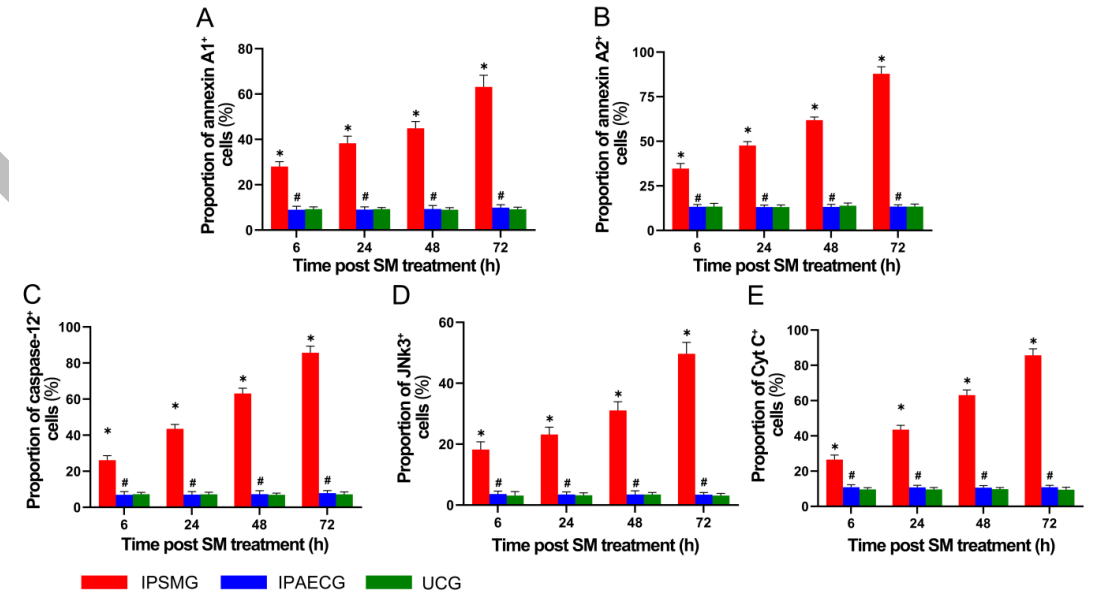

Figure 4. The proportion of annexin A1- (A), annexin A2- (B), caspase-12- (C), JNK3- (D), and Cyt C- (E) positive cells in the alveolar septa of rats via intraperitoneal administration. Figure 2 exhibits the rat treatment protocol. Data are mean±SD, n=8. *p<0.05, compared with IPECG and UCG. #p>0.05, compared with untreated control group (UCG).

Published by Tehran University of Medical Sciences (http://ijaai.tums.ac.ir)

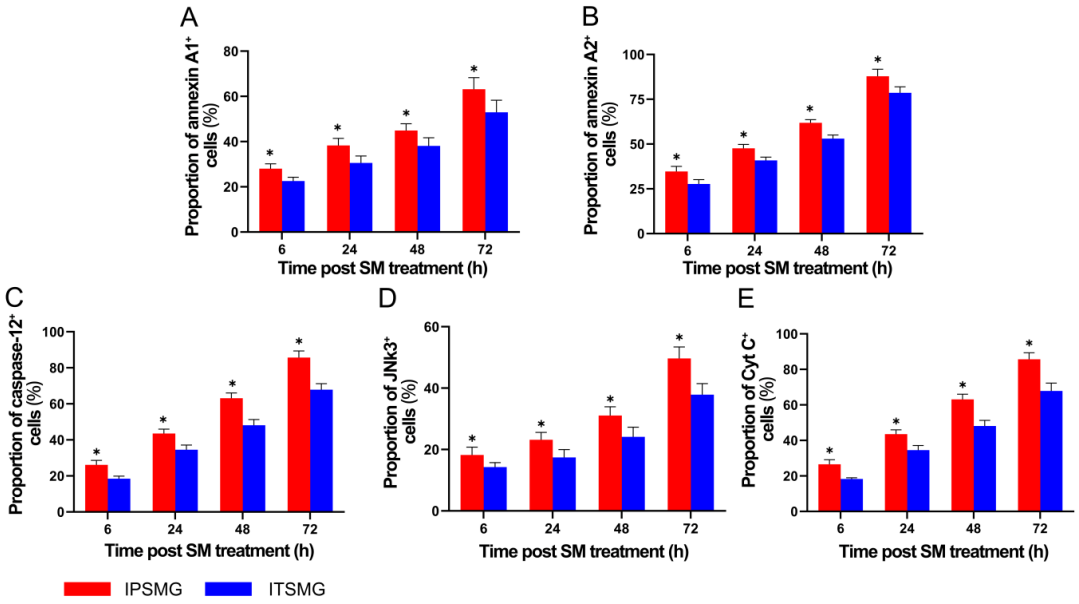

Figure 5. The proportion of annexin A1- (A), annexin A2- (B), caspase-12- (C), JNK3- (D), and Cyt C- (E) positive cells in the alveolar septa of rats through two routes. Figures 1 and 2 depict the rat treatment protocol. Data are mean ± SD, n = 8. *p<0.05, compared with the ITSMG.

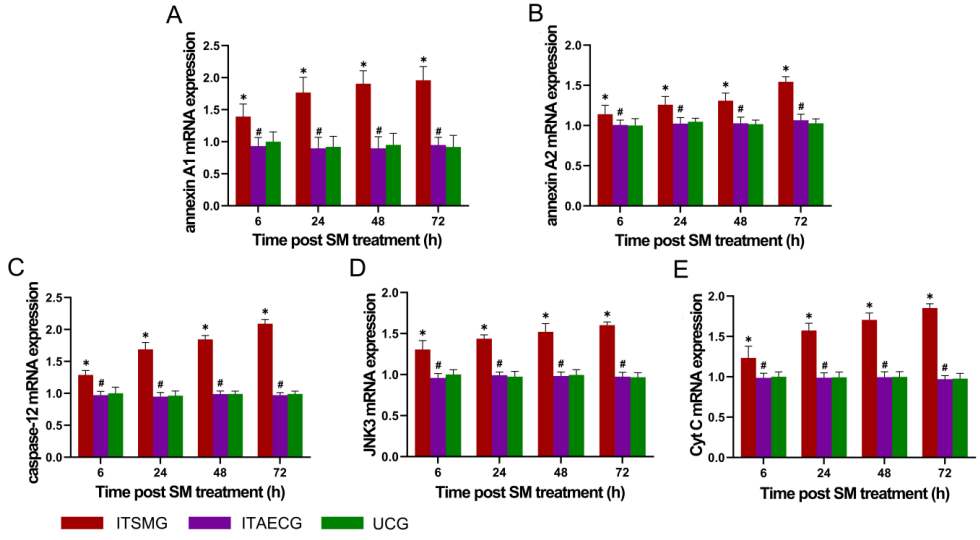

Figure 6. mRNA expression of annexin A1- (A), annexin A2- (B), caspase-12- (C), JNK3- (D), and Cyt C- (E) in the alveolar septa of rats via intratracheal administration. Figure 1 depicts the rat treatment protocol. Data are mean ± SD, n=8. *p<0.05, compared with ITECG and UCG. #p>0.05, compared with untreated control group (UCG). Abbreviation: mRNA, messenger ribonucleic acid.

Published by Tehran University of Medical Sciences (http://ijaai.tums.ac.ir)

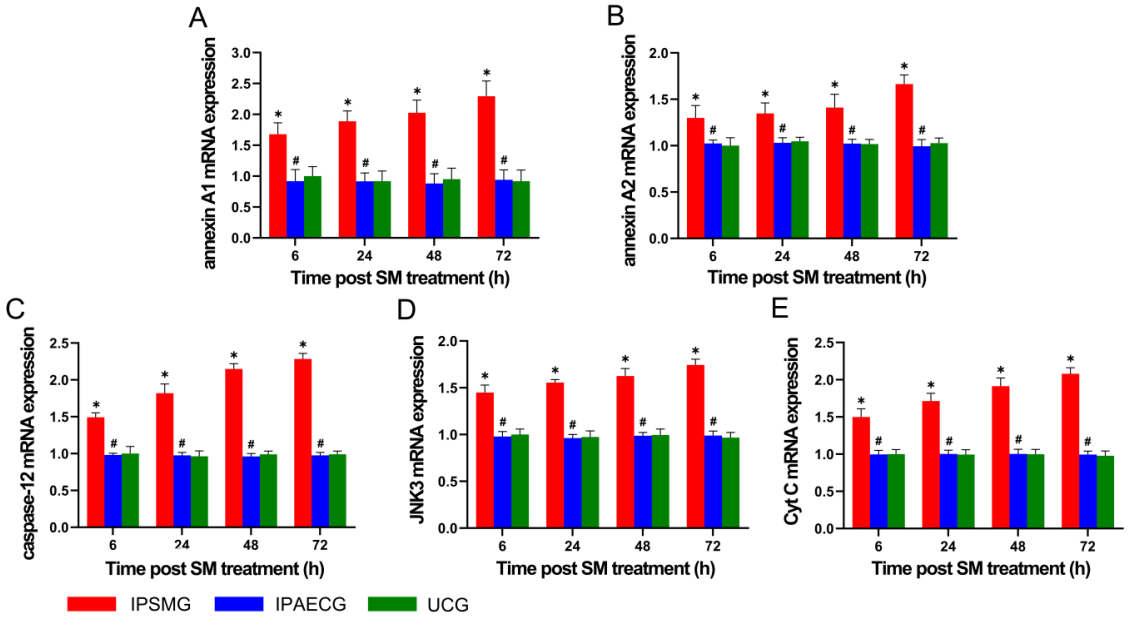

Figure 7. mRNA expression of annexin A1- (A), annexin A2- (B), caspase-12- (C), JNK3- (D), and Cyt C- (E) in the alveolar septa of rats via intraperitoneal administration. Figure 2 shows the rat treatment protocol. Data are mean ± SD, n=8. $^{*}p<0.05$, compared with IPAECG and UCG. $^{\#}p>0.05$, compared with untreated control group (UCG).

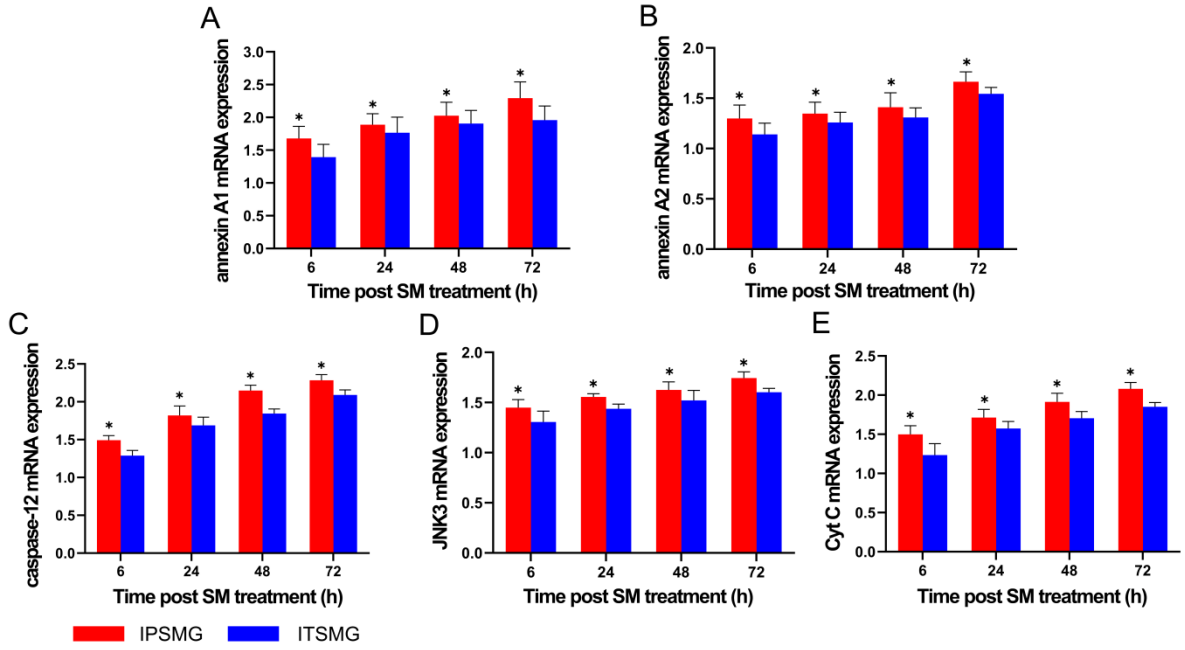

Figure 8. mRNA expression of annexin A1- (A), annexin A2- (B), caspase-12- (C), JNK3- (D), and Cyt C- (E) in the alveolar septa of rats through two routes. Figures 1 and 2 show the rat treatment protocol. Data are mean±SD, n=8. $^{*}p<0.05$, compared with ITSMG.

DISCUSSION

Apoptosis represents a major pathogenic mechanism underlying tissue damage in acute lung injury.[12] To comprehensively evaluate apoptotic processes in SM-induced pulmonary injury, we employed a multi-modal approach combining TUNEL assays for apoptotic cell detection, immunohistochemical labeling for protein localization and expression, and quantitative real-time PCR for gene expression analysis. TUNEL assays and immunohistochemical analyses revealed marked elevations in both apoptotic cell populations and apoptosis-related protein expression within SM-exposed groups relative to all control conditions. These findings corroborate and extend previous observations regarding SM-induced apoptotic pathways in pulmonary tissue. Research has shown that SM triggers programmed cell death through two distinct pathways: the mitochondrial pathway and the death receptor pathway.[13,14] In a key study, Steinritz et al[15] demonstrated human bronchial epithelial cells exposed to SM and observed clear indicators of apoptosis, including increased TUNEL staining and poly (ADP-ribose) polymerase fragmentation. These findings were consistent with the activation of effector caspases-3/7. Earlier studies using human bronchial epithelial cell lines have similarly demonstrated that SM induces apoptosis, consistent with findings in pulmonary cells. These cell lines provide a well-established model for studying the upper respiratory tract, which represents a primary target site for SM exposure.[16] These findings establish apoptosis as a central mechanism in SM-induced cell death. The methods outlined here offer a versatile approach for identifying therapeutic compounds that can modulate apoptotic pathways to alleviate lung damage, providing a promising avenue for targeted therapeutic intervention.

TUNEL staining revealed a significant increase in apoptotic cells in both intraperitoneal and intratracheal SM-exposed groups compared to control groups. These results align with findings by Mosayebzadeh et al[17] who demonstrated caspase-dependent apoptosis (activated caspase-3) in lung tissue. The brown nuclei observed in the TUNEL assay represent characteristic features of apoptosis, displaying condensed chromatin and nuclear fragmentation that clearly distinguish apoptotic cells from necrotic cells with non-specific DNA damage. Ultrastructural analysis revealed distorted mitochondrial cristae and ribosomal detachment from the rough endoplasmic reticulum, with ribosomes subsequently dispersing throughout the cytoplasm.[11] These structural changes confirm that apoptosis represents a key mechanism in acute pulmonary injury induced by SM exposure via both intraperitoneal and intratracheal pathways. The extent of apoptosis showed a positive correlation with both dose and duration of SM exposure. Our results are consistent with findings by Blaha et al,[18] which supports the reliability of TUNEL assays for confirming electron microscopy results.

Annexin A1 is primarily localized in the cytosol but translocates to the plasma membrane in response to cellular signals. It plays critical roles in regulating diverse physiological processes, including the modulation of inflammatory responses, cell proliferation and differentiation, and execution of apoptosis in vivo.[19] Elevated annexin A1 levels have been shown to influence caspase-3 and caspase-9 signaling, which are essential components of the apoptotic pathway.[20,21] In this study, increased annexin A1 levels were observed in epithelial cells of the alveolar septa and positively correlated with both the proportion of apoptotic cells and mRNA expression levels. These findings suggest that apoptosis occurs through a mitochondrial-dependent pathway in SM-induced pulmonary injury following both intraperitoneal and intratracheal exposure in rats. The results indicate that annexin A1 plays a crucial role in mediating apoptosis, likely through its interaction with mitochondrial signaling cascades.

Previous studies have shown that annexin A2 directly binds to p53, suppressing its transcriptional activity and promoting proteasomal degradation. Consequently, annexin A2 degradation leads to elevated p53 protein levels and increased downstream target gene expression.[22,23] Li et al[24] demonstrated that RNAi-mediated downregulation of annexin A2 in vitro resulted in p53 upregulation and mitochondrial membrane depolarization, both key events in the mitochondrial-dependent apoptotic pathway. Additionally, research using embryonic fibroblasts from p53-deficient and heterozygous mice has revealed heightened susceptibility to SM-induced DNA damage and cellular toxicity.[25] Our immunostaining analysis demonstrated increased protein and gene expression levels in alveolar epithelial cells using specific molecular markers. These collective findings indicate that p53 functions as a critical protective factor against SM-induced damage by controlling DNA repair mechanisms and apoptotic signaling pathways. This compensatory response likely functions to restore the critical equilibrium between pro-

Published by Tehran University of Medical Sciences (http://ijaai.tums.ac.ir)

apoptotic and anti-apoptotic signaling pathways that SM exposure disrupts.

The JNK3 signaling cascade serves as a central mediator of stress-induced apoptotic responses through dual mechanistic pathways. External stimuli activate death receptors like Fas, while internal cellular damage triggers mitochondrial outer membrane permeabilization via Bax/Bak proteins.[26] Upon activation, JNK-mediated phosphorylation simultaneously executes two critical functions: it enhances pro-apoptotic protein activity by promoting Bad, Bim, and Bid translocation to the mitochondria and facilitating membrane disruption, while simultaneously neutralizing protective factors through phosphorylation-dependent degradation of anti-apoptotic proteins such as Bcl-2 and Bcl-xL. Our experimental analysis revealed substantial elevation in both JNK3 mRNA transcript levels and JNK3-immunoreactive cell populations across intraperitoneal and intratracheal SM exposure groups. These elevated JNK3 concentrations indicate robust activation of mitochondrial-mediated apoptotic machinery through a coordinated regulatory mechanism. Specifically, JNK3 signaling appears to orchestrate cellular death by simultaneously promoting transcriptional enhancement of death-inducing Bax and Bak proteins while triggering post-translational suppression of survival factors Bcl-2 and Bcl-xL, thereby creating a decisive shift toward apoptotic execution.[27]

Cellular stress within the endoplasmic reticulum initiates a lethal signaling cascade when ER-localized caspase-12 becomes activated. This activation triggers sequential molecular events: Bid protein cleavage followed by caspase-9 recruitment, which converges on cytoplasmic caspase-3 to execute the final apoptotic program.[28] Our investigation revealed considerable increases in caspase-12 expression across multiple levels, both protein abundance (quantified through immunopositive cell analysis) and corresponding transcript levels, within alveolar epithelial tissue. These coordinated elevations occurred consistently across both systemic (intraperitoneal) and direct pulmonary (intratracheal) SM delivery methods, establishing caspase-12 as a primary stress-response mediator activated by SM-induced cellular damage. Our findings align with established research by Fakhrinnisa et al[29] and Peyrou et al,[30] who documented similar ER stress-mediated caspase-12 activation in cisplatin-induced renal toxicity models. The convergence of these independent studies with our current observations establishes caspase-12 as a critical executor of ER stress-triggered apoptotic pathways, operating through Bid-mediated recruitment of the caspase-9/caspase-3 death machinery.[31] Within mitochondrial bioenergetics, cytochrome c functions as a mobile electron carrier that facilitates energy transfer by receiving electrons from respiratory complex III and subsequently delivering them to cytochrome c oxidase (complex IV). This dual role positions cytochrome c as both an essential component of cellular respiration and a pivotal apoptotic signalling molecule upon mitochondrial membrane disruption.

The classical intrinsic apoptotic pathway, which originates within the mitochondria, is activated by various stimuli that cause Cyt C to be released from the mitochondria into the cytoplasm, where it initiates the activation of caspases.[32] In the mitochondrial electron transport chain, Cyt C functions as a soluble electron carrier, accepting electrons from Complex III and transferring them to Complex IV.[33] Consistent with the findings of Pohl et al, our data demonstrate elevated Cyt C levels in the cytosol of SM-exposed rat lungs, indicating mitochondrial outer membrane permeabilization and subsequent activation of pulmonary epithelial apoptosis.[34] These effects may be explained by the role of SM as DNA damage and oxidative stress trigger the mitochondrial apoptosis pathway. The release of mitochondrial Cyt C into the cytosol triggers apoptosome formation, leading to caspase-9 activation and subsequent cleavage of effector caspases (caspase-3/7), which mediate cell death by proteolytically degrading target proteins.[35]

Overall, this study shows that the expression of apoptosis-related proteins and genes in the alveolar septa increases progressively over time. Furthermore, the number of apoptotic cells was positively correlated with alveolar septal thickening, clinical ARDS severity, and patient mortality. The temporal pattern of apoptosis closely mirrored the trends observed for inflammatory response and oxidative stress reported in earlier studies.[8,9] Our findings also confirm that SM activates multiple apoptotic pathways. In the intrinsic pathway, annexin A1 activates caspase-3 and caspase-9, while p53 upregulates Bax, increasing mitochondrial outer membrane permeability, which promotes Cyt C release and triggers the caspase-9–dependent apoptotic cascade. In the extrinsic pathway, JNK upregulates the expression of suicide ligand expression, further

promoting apoptosis. Additionally, the ER stress-dependent pathway involves activation of caspase-12 by ER stress, which mediates apoptosis and contributes to pulmonary injury.

A key limitation of this study is the exclusive reliance on rat models to investigate SM-induced pulmonary injury. This limitation arose from technical constraints in experimental design, which confined model establishment to intratracheal instillation and intraperitoneal injection methods. Although we assessed changes in apoptosis-related proteins and gene expression linked to SM-induced cell death, no novel apoptotic mechanisms or signaling pathways were discovered. Moreover, this model represents acute high-dose exposure, which may not accurately reflect chronic low-level environmental exposures or be directly applicable to human risk assessment.

In conclusion, the comparative analysis of intraperitoneal and intratracheal SM exposure revealed critical differences in route-specific effects. At equivalent toxic doses, intraperitoneal injection induced a significantly greater number of apoptotic cells and higher expression of apoptosis-related proteins and genes in the alveolar epithelium. The data indicate that SM-induced apoptotic responses differ markedly based on the route of administration, systemic distribution, bioavailability, and pharmacokinetic properties. These findings highlight distinct exposure-pathway-specific variations in programmed cell death and emphasize the need for further research to assess the clinical relevance of these results in human SM exposure scenarios.

STATEMENT OF ETHICS

All experimental protocols were approved by the Animal Research Ethics Committee of the Institute of Academy of Military Medical Sciences, bearing the code of ethics CN.BJ.JSYXYJY.2024.1266.

FUNDING

This study was supported by the Military Logistics Project of China (Grant No. AWS17J008).

CONFLICT OF INTEREST

The authors declare no competing financial interests or personal relationships that could influence the work reported in this paper.

ACKNOWLEDGMENTS

We acknowledge the support of the Institute of Toxicology and Pharmacology, Academy of Military Medical Sciences, for their assistance in this research.

DATA AVAILABILITY

The datasets used and/or analyzed during the current study are available from the corresponding author on reasonable request.

AI ASSISTANCE DISCLOSURE

This study did not use AI assistance.

REFERENCES

1. Kumar R, Sinha DM, Lankau BR, Sinha NR, Tripathi R, Gupta S, et al. Differential gene expression and protein-protein interaction network profiling of sulfur mustard-exposed rabbit corneas employing RNA-seq data and bioinformatics tools. Exp Eye Res. 2023;235:109644.
2. Xiao Z, Liu F, Cheng J, Wang Y, Zhou W, Zhang Y. B-Raf inhibitor vemurafenib counteracts sulfur mustard-induced epidermal impairment through MAPK/ERK signaling. Drug Chem Toxicol. 2023;46(2):226-35.
3. Jost P, Muckova L, Pejchal J. In vitro stress response induced by sulfur mustard in lung fibroblasts NHLF and human pulmonary epithelial cells A-549. Arch Toxicol. 2020;94(10):3503-14.
4. Sabnam S, Rizwan H, Pal S, Pal A. CEES-induced ROS accumulation regulates mitochondrial complications and inflammatory response in keratinocytes. Chem Biol Interact. 2020;321:109031.
5. Zhao Z, Yan X, Li L, Shu Y, He J, Wang L, et al. Proliferating stem cells are acutely affected by DNA damage induced by sulfur mustard. DNA Cell Biol. 2022;41(8):716-726.
6. Jamshidi V, Halabian R, Saeedi P, Bagheri H, Nobakht Motlagh Ghoochani BF. Accelerating synergistic effects of preconditioned mesenchymal stem cells with Crocin and dexamethasone in pulmonary epithelial cells injury. Toxicol Res (Camb). 2023;12(3):369-80.
7. Sabnam S, Pal A. Relevance of Erk1/2-PI3K/Akt signaling pathway in CEES-induced oxidative stress regulates inflammation and apoptosis in keratinocytes. Cell Biol Toxicol. 2019;35(6):541-64.

8. Dan Yu, Bei YY, Li Y, Han W, Zhong YX, Liu F, et al. In vitro the differences of inflammatory and oxidative reactions due to sulfur mustard induced acute pulmonary injury underlying intraperitoneal injection and intratracheal instillation in rats. Int Immunopharmacol. 2017;47:78-87.
9. Jiang YY, Li ZS, Yu D, Xie JW, Zhu XJ, Zhong YX. Changes in inflammatory factors and protein expression in sulfur mustard(1LD50)-induced acute pulmonary injury in rats. Int Immunopharmacol. 2018;61:338-45.
10. Liu L, Hu XX, Zhang N, Zhong YX, Zhu XJ, Liu T. Oxidative stress reactions in rats with pulmonary injuries induced by sulfur mustard (1LD50). Hum Exp Toxicol. 2024;43:9603271241308772.
11. Hu XX, Zhang N, Zhong YX, Liu T, Zhu XJ. Mechanisms of apoptosis and pulmonary fibrosis resulting from sulfur mustard-induced acute pulmonary injury in rats. Int J Toxicol. 2025;44(4):314-27.
12. Neff TA, Guo RF, Neff SB, Sarma JV, Speyer CL, Gao HW, et al. Relationship of acute lung inflammatory injury to Fas/FasL system. Am J Pathol. 2005;166(3):685-94.
13. Rosenthal DS, Velena A, Chou FP, Schlegel R, Ray R, Benton B, et al. Expression of dominant-negative Fas-associated death domain blocks human keratinocyte apoptosis and vesication induced by sulfur mustard. J Biol Chem. 2003;278(10):8531-40.
14. Simbulan-Rosenthal CM, Ray R, Benton B, Soeda E, Daher A, Anderson D, et al. Calmodulin mediates sulfur mustard toxicity in human keratinocytes. Toxicology. 2006;227(1-2):21-35.
15. Steinritz D, Emmler J, Hintz M, Worek F, Kreppel H, Szinicz L, et al. Apoptosis in sulfur mustard treated A549 cell cultures. Life Sci. 2007;80(24-25):2199-201.
16. Sourdeval M, Lemaire C, Deniaud A, Taysse L, Daulon S, Breton P, et al. Inhibition of caspase-dependent mitochondrial permeability transition protects airway epithelial cells against mustard-induced apoptosis. Apoptosis. 2006;11(9):1545-59.
17. Mosayebzadeh M, Ghazanfari T, Delshad A, Akbari H. Evaluation of Apoptosis in the Lung Tissue of Sulfur Mustard-exposed Individuals. Iran J Allergy Asthma Immunol. 2016;15(4):283-8.
18. Blaha M, Kohl J, DuBose D, Bowers W Jr, Walker J. Ultrastructural and histological effects of exposure to CEES or heat in a human epidermal model. In Vitr Mol Toxicol. 2001;14(1):15-23.
19. Hasan M, Kumolosasi E, Jantan I, Jasamai M, Nazarudin N. Knockdown of Annexin A1 induces apoptosis, causing G2/M arrest and facilitating phagocytosis activity in human leukemia cell lines. Acta Pharm. 2021;72(1):109-22.
20. Vago JP, Nogueira CRC, Tavares LP, Soriani FM, Lopes F, Russo RC, et al. Annexin A1 modulates natural and glucocorticoid-induced resolution of inflammation by enhancing neutrophil apoptosis. J Leukoc Biol. 2012;92(2):249-58.
21. Li GW, He SH, Chang LJ, Lu H, Zhang HW, Zhang H, et al. GADD45α and annexin A1 are involved in the apoptosis of HL-60 induced by resveratrol. Phytomedicine. 2011;18(8-9):704-9.
22. Wu MH, Sun YQ, Xu FP, Liang YQ, Liu H, Yi YM. Annexin A2 silencing inhibits proliferation and epithelial-to-mesenchymal transition through p53-dependent pathway in NSCLCs. J Cancer. 2019;10(5):1077-85.
23. Wang CY, Chen CL, Tseng YL, Fang YT, Lin YS, Su WC, et al. Annexin A2 silencing induces G2 arrest of non-small cell lung cancer cells through p53-dependent and -independent mechanisms. J Biol Chem. 2012;287(39):32512-24.
24. Li DW, Qi XD, Zhang CH, Sun WP. Annexin A2 degradation contributes to dopaminergic cell apoptosis via regulating p53 in neurodegenerative conditions. Neuroreport. 2021;32(15):1263-8.
25. Inturi S, Tewari-Singh N, Jain AK, Roy S, White CW, Agarwal R. Absence of a p53 allele delays nitrogen mustard-induced early apoptosis and inflammation of murine skin. Toxicology. 2013;311(3):184-90.
26. Tournier C, Hess P, Yang DD, Xu J, Turner TK, Nimnual A, et al. Requirement of JNK for stress-induced activation of the cytochrome c-mediated death pathway. Science. 2000;288(5467):870-4.
27. Gurzov EN, Eizirik DL. Bcl-2 proteins in diabetes: mitochondrial pathways of β-cell death and dysfunction. Trends Cell Biol. 2011;21(7):424-31.
28. Hitomi J, Katayama T, Taniguchi M, Honda A, Imaizumi K, Tohyama M. Apoptosis induced by endoplasmic reticulum stress depends on activation of caspase-3 via caspase-12. Neurosci Lett. 2004;357(2):127-30.
29. Fakhrinnisa TA, Susilo I, Mustika A, Sofyan MS. Effect of intravenous glutamine on caspase-12 expression in the apoptosis of the glomerular epithelial cells of male rats exposed to cisplatin. Asian Pac J Cancer Prev. 2021;22(2):457-62.
30. Peyrou M, Hanna PE, Cribb AE. Cisplatin, gentamicin, and p-aminophenol induce markers of endoplasmic reticulum stress in the rat kidneys. Toxicol Sci. 2007;99(1):346-53.

31. Zhang Q, Liu J, Chen S, Liu J, Liu L, Liu G, et al. Caspase-12 is involved in stretch-induced apoptosis mediated endoplasmic reticulum stress. Apoptosis. 2016;21(4):432-42.
32. Brown GC, Borutaite V. Regulation of apoptosis by the redox state of cytochrome c. Biochim Biophys Acta. 2008;1777(7-8):877-81.
33. Pérez-Mejías G, Guerra-Castellano A, Díaz-Quintana A, De la Rosa MA, Díaz-Moreno I. Cytochrome c: surfing off of the mitochondrial membrane on the tops of complexes III and IV. Comput Struct Biotechnol J. 2019;17:654-60.
34. Pohl C, Papritz M, Moisch M, Wübbeke C, Hermanns MI, Uboldi C, et al. Acute morphological and toxicological effects in a human bronchial coculture model after sulfur mustard exposure. Toxicol Sci. 2009;112(2):482-9.
35. Sharma DR, Sunkaria A, Bal A, Bhutia YD, Vijayaraghavan R, Flora SJ, et al. Neurobehavioral impairments, generation of oxidative stress and release of pro-apoptotic factors after chronic exposure to sulphur mustard in mouse brain. Toxicol Appl Pharmacol. 2009;240(2):208-18.